PERGAMON

Solid State Communications 113 (2000) 147–151

solid state communications

www.elsevier.com/locate/ssc

On the metallic behavior of Co clusters

F. Aguilera-Granja[a,*], J.M. Montejano-Carrizales[a], J. Guevara[b,1], A.M. Llois[c,d]

[a]*Instituto de Física, "Manuel Sandoval Vallarta" Universidad Autónoma de San Luis Potosí, 78000 San Luis Potosí, S.L.P., Mexico*
[b]*Department of Chemistry, Boston University, Boston, MA 02215, USA*
[c]*Departamento de Físico, Comisión Nacional de Energía Atómica, Avda. del Libertador 8250, 1429 Buenos Aires, Argentina*
[d]*Departamento de Física, Facultad de Ciencias Exactas y Naturales, Universidad de Buenos Aires, Pab I, Ciudad Universitaria, (1429) Buenos Aires, Argentina*

Received 26 July 1999; accepted 25 September 1999 by C.E.T. Gonçalves da Silva

Abstract

The role of structure in the nonmetal–metal transition of Co clusters is investigated by performing calculations for different symmetries: hexahedral, octahedral and decahedral. This transition occurs when the density of states at the Fermi level exceeds $1/k_BT$ and the discrete energy levels begin to form a quasi-continuous band. The electronic structure is calculated including spd orbitals and spillover effects in a Hubbard Hamiltonian solved within the unrestricted Hartree–Fock approximation. We find that in small clusters ($N \leq 40$) the metallic behavior is strongly related to the geometrical structure of the cluster. We compare our results with those coming out of a simple Friedel's model.

Keywords: A. Insulators; A. Metals; A. Nanostructures

1. Introduction

Clusters of metallic elements have very interesting chemical and physical properties that are completely different from those of single atoms and bulk materials. Small clusters of metallic elements are insulators due to the discrete distribution of the electronic states. A transition from insulating (nonmetallic) to metallic behavior with increasing cluster size is expected [1–11]. Kubo et al. introduced a first theoretical criterion to identify this transition pointing out that it should occur when the average spacing between electronic levels becomes smaller than k_BT and the discrete energy levels begin to form a quasi-continuous band. In terms of the density of states (DOS) the transition takes place when at the Fermi level DOS exceeds $1/k_BT$.

The distribution of energy levels depends on the geometrical structure of the clusters and experimental information alone is not enough to determine it. Structure calculations are usually restricted to clusters of relatively small size, mainly $N \leq 20$ and the results of different theoretical calculations often do not coincide [12–16].

In this paper, we are interested in the nonmetal–metal transition of Co clusters. We use a self-consistent tight-binding method using spd orbitals to calculate the electronic density of states and apply Kubo's criterion to determine the critical cluster size. No experimental results are reported for small Co clusters and we are not aware of any first principles molecular dynamics calculations for the determination of geometrical structure in the literature. We perform then calculations for different possible geometries. Method of calculation and results are presented in Sections 1 and 3, respectively, and the conclusions in Section 4.

2. Method of calculation

2.1. Self-consistent calculations

A Hubbard tight-binding Hamiltonian with spd orbitals and parameters from bulk Co are used. The electronic structure is obtained by solving it in the unrestricted Hartree–Fock approximation. All many-body contributions appear in the diagonal spin dependent term $\varepsilon_{im\sigma}$ with respect

* Corresponding author. Fax: +48-13-38-74.
E-mail address: faustino@alpha2.ifisica.uaslp.mx (F. Aguilera-Granja)
[1] Permanent address: Escuela de Ciencia y Tecnología, University of San Martín, San Andrés, Prov. de Buenos Aires, Argentina.

0038-1098/00/$ - see front matter
PII: S0038-1098(99)00460-3

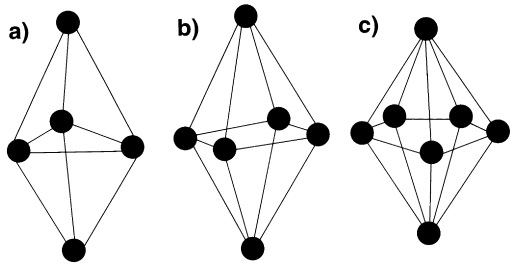

Fig. 1. Set of basic polyhedra used in this work: (a) hexahedron; (b) octahedron; and (c) decahedron.

to ε_{im}^{0}, given by:

$$\sum_{m'}\left(U_{imm'}\Delta\eta_{im'} - \sigma\frac{J_{imm'}}{2}\mu_{im'}\right) + \Delta\varepsilon_i^{\mathrm{MAD}}, \qquad (1)$$

where $\Delta\eta_{im'}$ is the electron occupation difference with respect to bulk paramagnetic values, per orbital in the ith atom. $\mu_{im'}$ is the magnetization per orbital, and $\Delta\varepsilon_i^{\mathrm{MAD}}$ is the Madelung term. Parametrization and treatment of electron spillover at the cluster surface are done as in Refs. [17–20].

The Hamiltonian is solved self-consistently diagonalizing at each step the majority and minority matrices and electronic occupations per orbital, spin, and atom are obtained. A Gaussian broadening (0.02 eV) was used to get a continuous representation of the DOS with the aim to use the Kubo's criterion.

The total density of states at the Fermi level, $\mathscr{D}_N(E_F) = \sum_{im\sigma}\mathscr{D}_{im\sigma}(E_F)$ results also from the self-consistent calculation and we have used it to determine the nonmetal–metal transition according to Kubo's criterion [8], $\mathscr{D}_N(E_F) > 1/k_B T$, for the development of metallic character.

Our one-particle Hamiltonian neglects correlation effects beyond the mean field approximation and also the dependence of the DOS with temperature. The previous assumption was adequate in the case of Ni for temperatures below 640 K [21,22] we expect that this approximation also holds for Co since all the temperature we are going to consider are below this value. We are not aware of any finite temperature calculation in the case of Co bulk systems. The changes of the DOS are expected to occur only as a consequence of the finite size and geometry of the clusters. It is also important to mention that we are assuming that there is no structural transition along the temperature range considered here.

The simplest model for the DOS of d band systems is the one due to Friedel, in this model sp orbitals are not considered and a rectangular shape is assumed. A second moment approximation introduces the dependence of bandwidth on local average coordination [21,25]. In this work, we also include the calculation based on Friedel's model to be used as a reference.

Since we are interested in the general tendencies of the nonmetal–metal transition temperature, it is important to mention, before showing the results, that the main conclusions and tendencies of this calculation are not going to change qualitatively if some other value for the width of the Gaussian broadening is used.

2.2. Generation of geometrical structures

The geometries studied here are: hexahedral (Hexa), octahedral (Octa), and decahedral (Deca). The polyhedra or seeds are shown in Fig. 1 and their geometrical characteristics are given in Table 1. To build a geometrical family starting from these seeds, we add atoms on top of the center of each face with the restriction that they have to be equidistant from all atoms forming that face. We refer to these sites as available ones. However, it is not always possible to put atoms over all the available sites without getting bonds,

Table 1
Geometrical characteristics of the clusters used in this work. The upper panel corresponds to the basic polyhedra and the lower part to the different saturated polyhedra

Polyhedron	N_v [a]	N_f [b]	N_a [c]	N_p [d]	N_{max} [e]	Coordination numbers						
						3	4	5	6	7	8	12
Hexa	5	6	6	0	11	2	3					
Octa	6	8	8	0	14		6					
Deca	7	10	10	0	17		5		2			
Hexam	11	18	18	6	23		6		2		3	
Octam	14	24	0	0	14	8				6		
Decam	17	30	30	13	34			10		5		2

[a] N_v: number of vertices.
[b] N_f: number of faces.
[c] N_a: number of available sites.
[d] N_p: number of prohibited sites.
[e] N_{max}: maximum number of sites.

Table 2
Geometrical characteristics of some of the clusters grown by the method described in the text

Polyhedron	N_v	N_f	Coordination numbers							
			2	3	4	5	6	7	8	12
Hexa + 1	6	8		2	2	2				
Octa + 1	7	10		1	3	3				
Deca + 1	8	12		1	3	2	1	1		
Deca(5)	5	–	5							
DI	19	30					12		5	2
Hexa + 2	7	10			5	2				
Hexa + 2	7	10		2	2	2	1			
Hexa + 2	7	10		3		3	1			

which are much shorter than the first-neighbor distance. In that case, we neglect one of these sites (forbidden site). In Table 1, we give the number of available N_a (forbidden N_p) sites. For a particular polyhedron, at this stage of the growing process, the maximum number of atoms N_{max} in the cluster is given by adding to the number of atoms of the basic polyhedron (N_v), the number of available sites (N_a) and subtracting the number of forbidden ones (N_p). The tolerance for the nearest-neighbor distance is in the range from 0.866 to 1.2 (in units of the bulk values). Columns 7 to 13 contain the local coordination number for each one of the polyhedra. In this table general geometrical characteristics of the resultant polyhedra are also given. In Table 2, we present the coordination evolution for some clusters generated along the growth process. To get the hexahedron plus one atom (Hexa + 1) cluster, we add one top site. There are six possibilities for it and they are all equivalent. The same occurs for the Octa + 1 and Deca + 1 clusters. For the Hexa + 2 cluster there are 15 arrays, but only three of them are nonequivalent: (i) two top sites over faces with a common edge that joins two four-fold coordinated sites; (ii) two top sites over faces with a common edge that joins three-fold and a four-fold coordinated sites; (iii) two top sites over two faces with a common four-fold coordinated site. It is worth noting that even if atoms with different local coordination are added, the cluster average coordination is the same in all three cases. For the octahedral family the way to get clusters with more than 14 atoms is by taking sites on a fcc array. The growth process is described in detail in Refs. [23,24].

It is important to mention that no experimental results for the geometrical shapes of Co clusters are available in the literature [16]. On the other hand, we are not aware of any first principles molecular dynamics calculations for them. Because of this we study those clusters shown in Fig. 1, however, it is worth notice that the clusters shown in Fig. 1 have been found to be the ground state structures of Co clusters by doing symbiotic algorithm calculations [27].

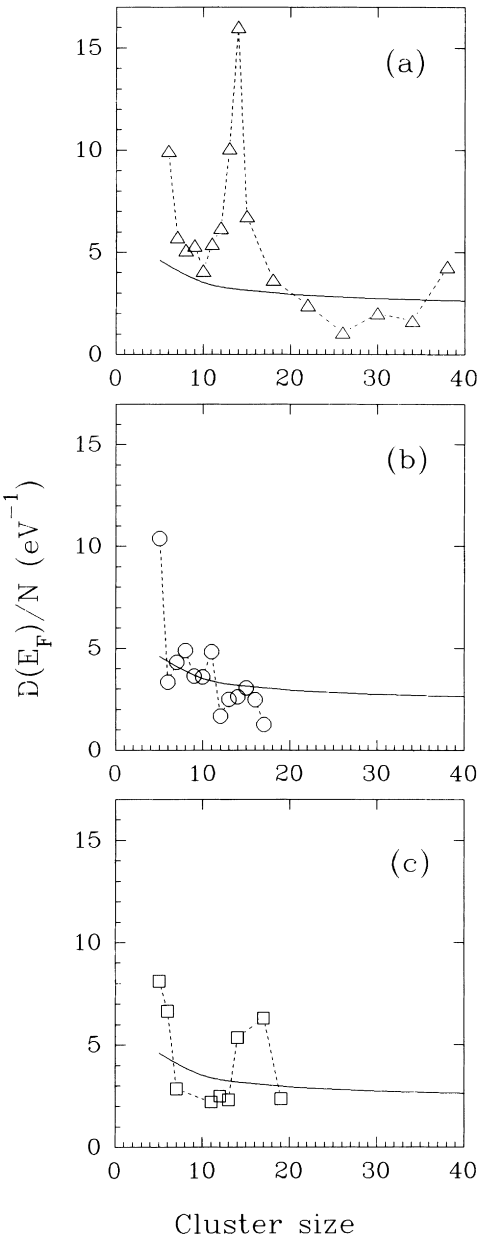

Fig. 2. Total density of electronic states at the Fermi level as a function of the cluster size for the three different geometries studied here: (a) octahedral; (b) hexahedral; and (c) decahedral. The continuous line gives the results of Friedel's rectangular d-band model. Notice that Friedel's model describes the general trends of $\mathcal{D}(E_F)/N$ as a function of the cluster size.

3. Results

In Fig. 2, the values of the density of states at the Fermi level for the three different symmetries considered here as a function of cluster size are shown. In (a) for the octahedral, (b) for the hexahedral and (c) for the decahedral based like

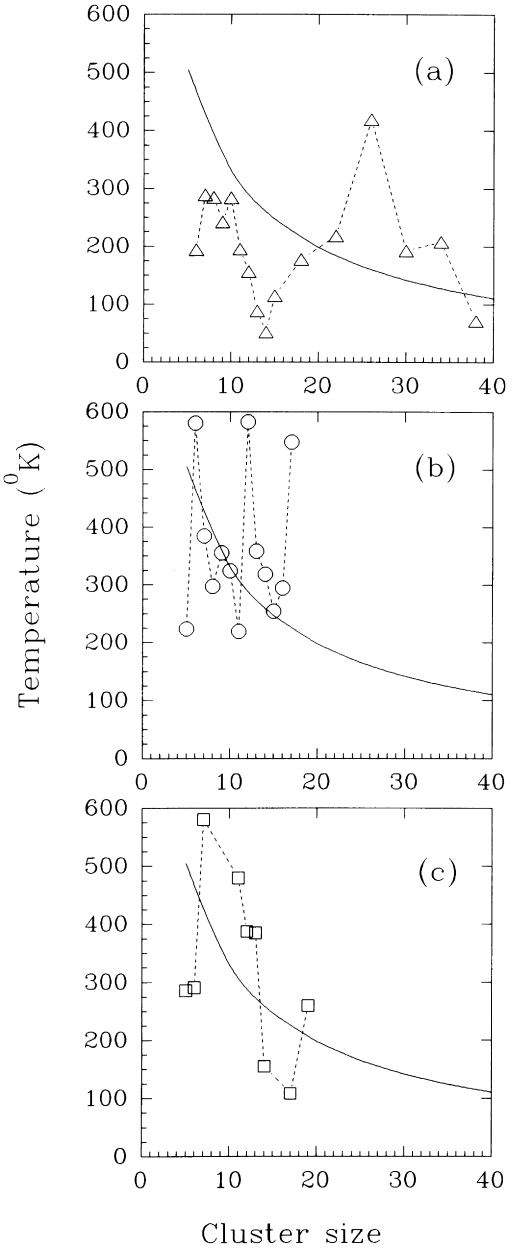

Fig. 3. The calculated nonmetal–metal phase diagram of the Co clusters using Kubo's criterion for the three different geometries studied here: (a) octahedral; (b) hexahedral; and (c) decahedral. The continuous line corresponds to the simple Friedel's rectangular d-band model.

clusters. We include as a reference the results of the Friedel-like model, assuming in this last case an fcc structure for the clusters [21,25]. The octahedral clusters (a) show an overall decreasing tendency in the $\mathscr{D}_N(E_F)/N$, with maxima for closed structures, that is $N = 6$, 14 and 38, and minima when half of the sites are empty in the geometrical structure,

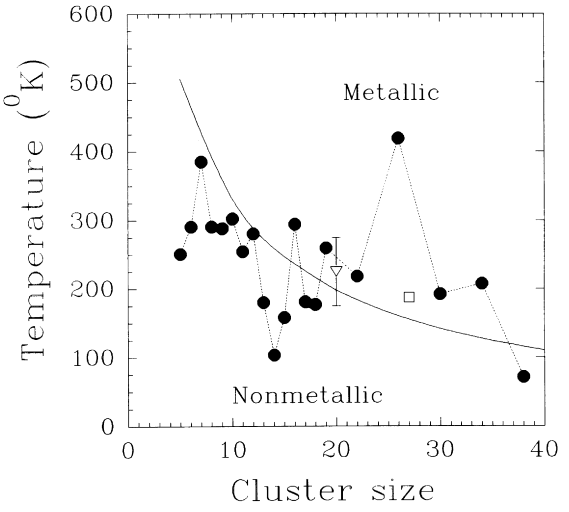

Fig. 4. Average nonmetal–metal phase diagram of the Co clusters studied here is shown (full circles). In this diagram, the region below the boundary describes nonmetallic clusters while the region above it corresponds to the metallic state. The open triangle is derived from Ref. [28] and the square from Ref. [29]. The continuous line corresponds to Friedel's rectangular d-band model.

$N = 10$ and 26. The hexahedral clusters (b) show again an overall decreasing tendency with maxima for closed shell clusters ($N = 5, 11$) and also for those at half-filled shells. The decahedral case (c) once more present an overall decreasing tendency, however in this case the closed shell structures are those that present minima while maxima appear at open shell structures.

This self-consistent tight-binding calculation gives $\mathscr{D}_N(E_F)/N$ with more structure than Friedel's model, the differences being particularly large in the small cluster region. Considering that Friedel's model only takes into account the average coordination, this means that it is the increase of the average coordination which gives rise to the monotonic decreasing behavior of $\mathscr{D}_N(E_F)/N$ as a function of N.

In Fig. 3 we show the phase diagram for the nonmetal–metal transition calculated using Kubo's criterion for the three different symmetries considered here. Friedel's approximation is shown with a continuous line, and it describes an average transition behavior from nonmetallic to metallic regime in the direction of increasing temperature.

The results coming out of the quantum mechanical calculation show large deviations with respect to simple Friedel's model and puts in evidence the importance of considering clusters geometry and orbital symmetry. Octahedral clusters of closed geometrical structure, $N = 6$, 14 and 38, become metallic for relatively low temperatures whereas those with open shell structure, $N = 10$ and 26, require higher temperature to go through the transition. In this case the closed shell structure favors the metallic behavior. In the hexahedral

case (b), the metallic behavior is favored both by closed shell structures ($N = 5, 11$) and by half-filled shell structure. For the decahedral case (c), we have a completely different behavior than in the previous cases, the metallic behavior being reached at lower temperatures for open shell geometrical structures.

In Fig. 4 we also show a phase diagram after averaging the results of the three symmetries and assuming a mixing of them with equal probability. The results of Friedel's model are plotted as well and should become better with growing cluster sizes. We are not aware of any direct experimental measurement of nonmetal–metal transition in Co clusters, since most of the experimental results are for other systems [26]. However, based on measurements of Ionization Potential (IP) and its deviation from the Conducting Spherical Droplet (CSP) model [28] one can do a first and rough estimation of critical cluster sizes for the nonmetal–metal transition [21,25]. We have made this estimation for two experimental values of IP obtained by Parks [29] and Yang [30]. The results are shown in Fig. 4 corresponding the triangle to Parks' experiment and the square to Yang's. For the latest experiment we estimate the internal cluster temperature by considering the way in which the clusters were prepared [30]. We obtain a good agreement between our calculation and the experimentally derived results.

4. Conclusions

We have studied the nonmetal–metal transition of Co clusters grown in different geometries. A self-consistent tight-binding Halmitonian which includes spd valence electrons and spillover effects solved in the Hartree–Fock approximation has been used to calculate the electronic density of states. Kubo's criterion was used to calculate the nonmetal–metal phase diagram. We find that the metallic behavior of small Co clusters ($N \leq 40$) is strongly dependent on the geometrical structure of the cluster. For octahedral clusters metallic behavior is reached at lower temperatures for closed shell structures than for the open ones. Hexahedral clusters reach metallic behavior at lower temperatures for both close and half-filled shell structures. On the contrary decahedral clusters show metallic behavior at lower temperatures for open shell structures. Qualitative agreement with experimental results derived from IP measurements is satisfactory.

Acknowledgements

We acknowledge to the Consejo Nacional de Ciencia y Tecnología (México) Grants No. 6-25851-E and 4920-E9406, and A.M.L. to Consejo Nacional de Investigaciones Científicas y Técnicas, to SECyT PICT 03-00105-02043, and to Fundación Sauberan.

References

[1] H. Fröhlich, Physica (Utrecht) 4 (1937) 406.
[2] P.N. First, J.A. Stroscio, R.A. Dragoset, D.T. Pierce, R.J. Celotta, Phys. Rev. Lett. 63 (1989) 1416.
[3] K. Rademann, B. Kaiser, U. Even, F. Hensel, Phys. Rev. Lett. 59 (1987) 2319.
[4] H. Haberland, H. Kornmeier, H. Langosch, M. Oschwald, G. Tanner, J. Chem. Soc. Faraday Trans. 86 (1990) 2473.
[5] F. Yonezawa, S. Sakamoto, F. Wooten, J. Non-Cryst. Solids 117/118 (1990) 477.
[6] F. Yonezawa, H. Tanikawa, J. Non-Cryst. Solids 205–207 (1996) 793.
[7] G.K. Wertheim, Z. Phys. D 12 (1989) 319.
[8] R. Kubo, A. Kawabata, S. Kobayashi, Ann. Rev. Mater. Sci. 14 (1984) 49.
[9] G. Pastor, P. Stampfli, K.H. Bennemann, Phys. Scripta 38 (1988) 623.
[10] G. Pastor, P. Stampfli, K.H. Bennemann, Europhys. Lett. 7 (1988) 419.
[11] J. Zhao, X. Chen, G. Wang, Phys. Rev. B 50 (1994) 15424.
[12] P. Ballone, R.O. Jones, Chem. Phys. Lett. 233 (1995) 632.
[13] O.B. Chiristensen, M.L. Cohen, Phys. Rev. B 47 (1993) 13643.
[14] M.J. López, J. Jellinek, Phys. Rev. A 50 (1994) 1445.
[15] S.K. Nayak, S.N. Khanna, B.K. Rao, P. Jena, J. Phys. Chem. A 101 (1997) 1072.
[16] J. Guevara, A.M. Llois, F. Aguilera-Granja, J.M. Montejano-Carrizales, Solid State Commun. 111 (1999) 335.
[17] J. Guevara, F. Parisi, A.M. Llois, M. Weissmann, Phys. Rev. B 55 (1997) 13283.
[18] O.K. Andersen, O. Jepsen, Phys. Rev. Lett. 53 (1984) 2471.
[19] O.K. Andersen, O. Jespen, D. Gloetzel, in: F. Basani, F. Fumi, M. Tosi (Eds.), Highlights of Condensed Matter Theory, North-Holland, Amsterdam, 1995.
[20] T. Bandyopadhyay, D.D. Sarma, Phys. Rev. B 39 (1989) 3517.
[21] F. Aguilera-Granja, S. Bouarab, A. Vega, J.A. Alonso, J.M. Montejano-Carrizales, Solid State Commun. 104 (1997) 635.
[22] W. Nolting, W. Borgiel, V. Dose, Th. Fauster, Phys. Rev. B 40 (1989) 5015.
[23] J.M. Montejano-Carrizales, F. Aguilera-Granja, J.L. Morán-López, NanoStructured Materials 8 (1997) 269.
[24] F. Aguilera-Granja, J.M. Montejano-Carrizales, J.L. Morán-López, Solid State Commun. 107 (1998) 25.
[25] F. Aguilera-Granja, J.M. Montejano-Carrizales, J.A. Alonso, in: J.L. Morán-López (Ed.), Current Problems in Condense Matter, Plenum, New York, 1998, p. 109.
[26] W.P. Halperin, Rev. Mod. Phys. 58 (1986) 553.
[27] J.L. Rodríguez-López, private communication.
[28] D.M. Wood, Phys. Rev. Lett. 46 (1981) 749.
[29] E.K. Parks, T.D. Klots, S.J. Riley, J. Chem. Phys. 92 (1990) 3813.
[30] S. Yang, M.B. Knickelbein, J. Chem. Phys. 93 (1990) 1533.